

Correspondence

Whirligig beetle uses lift-based thrust for fastest insect swimming

Yukun Sun¹, Jena Shields², and Chris Roh¹

Whirligig beetles (*Gyrinidae*) are the fastest-swimming insects. The one-centimeter long aquatic beetle can reach a peak acceleration of 100 m s^{-2} and a top velocity of 100 body lengths per second. Previous studies have suggested that drag-based thrust by their hind legs is responsible for their propulsion^{1–4}. For the drag-based thrust to be effective, however, the leg stroke velocity must exceed the swimming velocity. Therefore, for fast-swimming whirligigs, it is unlikely that the drag-based thrust is the main source of acceleration⁵. Here, we demonstrate that lift-based thrust enables the rapid swimming of the whirligigs.

For their life devoted to the water surface, whirligig beetles have evolved flat oar-like mid and hind legs, the latter of which plays a more important role in fast swimming. To understand how hind legs generate the necessary thrust, untethered forward swimming *Dineutus discolor* ($N = 3$; Figure 1A) were filmed at two camera angles. We analyzed two videos of each of the three different straight-moving beetles with non-zero initial velocity. Analysis of this footage allowed simultaneous measurement of body and leg kinematics (Figure 1D,E; see Supplemental information).

Their body kinematics show a rapid acceleration and fast speed (Figure 1G). For such a feat, in addition to accelerating the body mass ($69.5 \pm 1.6 \text{ mg}$), the hind legs need to provide enough force to overcome hydrodynamic drag (form, added mass, and wave drag)^{2,3}. Using the body kinematics data, the required thrust is calculated and shown in Figure 1F (see Supplemental information). The average thrust required during the power stroke was $3.9 \pm 1.7 \text{ mN}$.

To understand how the legs generate the required propulsive thrust, simultaneously measured leg kinematics were analyzed. For the analysis, we followed previous studies' three phase division of the whirligig's leg stroke: extension, power-stroke, and recovery-stroke phases¹. During the extension phase, the leg laterally unfolds and rotates about the leg axis, which orients the oar-like blade orthogonal to the water surface. The power stroke ensues,

wherein the pair of hind legs move synchronously (for the forward thrust) in a three-dimensional trajectory to propel the beetle (Figure 1C,D). During the power stroke, the hind legs continue to rotate about their leg axes with their hairs unfolding. At the end of the power stroke, the hind legs retract in the recovery stroke phase. Here, we focus our analysis on the power stroke phase, which accounts for $72.2 \pm 8.7 \%$ of the total impulse.

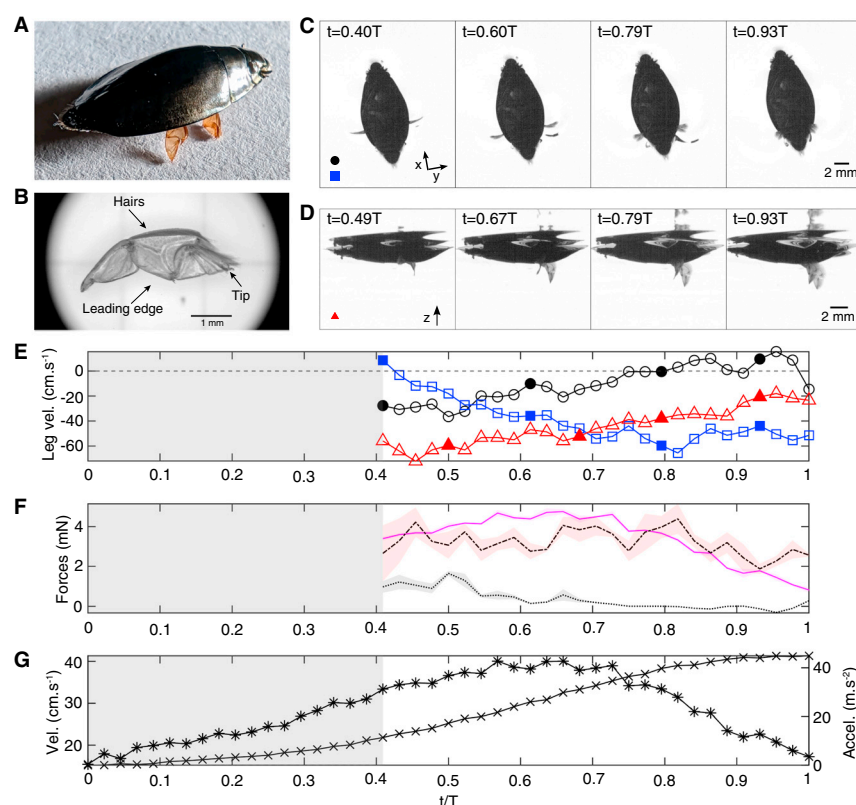


Figure 1. Morphology, kinematics, and force estimation of whirligig beetle accelerating in free swimming.

(A) Side view of a whirligig beetle on land. (B) Image of a dissected right hind leg. The hair is folded and attached to the trailing edge. (C) Selected bottom view (see also Video S1) of the leg kinematics of a free-swimming beetle in the power stroke phase. The legs were subjected to considerable inward motions towards the centerline of the body. The coordinate system, in which x is parallel to the longitudinal axis and y is parallel to the transverse axis of the beetle, is shown. (D) Selected side view (see also Video S1) of the leg kinematics of the free-swimming beetle. The positive z direction is shown. The legs were subjected to considerable downward motion. See also Figure S2. (E) Tip velocities of the hind leg in the power stroke phase. Black circles, u ; blue squares, v ; red triangles, w . The velocities (u , v , w) are associated with the coordinate system (x , y , z). The closed circles and squares correspond to the frames in (C). The closed triangles correspond to the frames in (D). Dashed line, zero-velocity baseline. See also Figure S2. (F) Estimated forces based on leg and body kinematics in the power stroke phase. Magenta solid line, thrust required. Dash-dotted line, lift-based thrust. Dotted line, drag-based thrust. The error (one standard deviation) in force estimated is enveloped by shaded region (magenta, thrust required; red, lift-based thrust; grey, drag-based thrust). (G) Body velocity (crosses) and acceleration (asterisks) during the full acceleration phase. The region shaded in grey represents the extension phase. The data shown here were derived from position tracking with a four-point interval ($\Delta = 4$; see also Supplemental information). See also Figure S2.

To generate positive drag-based thrust, the hind leg must create a backward motion (parallel and opposite to the swimming direction) relative to the surrounding fluid rather than to the body⁵. This motion corresponds to u , the longitudinal component of the leg tip velocity relative to water. The temporal variation of u shows that it fluctuated around zero at $-3.7 \pm 5.8 \text{ cm s}^{-1}$ during the power stroke (Figure 1E and Figure S2C–G in the Supplemental information). We estimated the average drag-based thrust to be $0.14 \pm 0.19 \text{ mN}$ (see Supplemental information). The average ratio between drag-based thrust to thrust required was -0.04 ± 0.20 . The resulting drag-based thrust is therefore insufficient for the large thrust that their rapid swimming demands; the hydrodynamic thrust associated with the other components of the leg velocity needs further examination.

Lift is the hydrodynamic force orthogonal to the object's motion relative to fluid. Thus, the vertical (z -axis) and transverse (y -axis) leg motions against water could generate lift force in the direction of the forward thrust (i.e. lift-based thrust). The continued rotation of the hind leg about the leg axis orients the oar blade's angle of attack (AoA; the angle between the relative freestream flow and the width/chord of the hind leg) amenable for lift-based thrust generation. During the power stroke, the hind legs moved downward ($-z$) and inward ($-y$) towards the body centerline (Figure 1E; $w = -47.8 \pm 11.7 \text{ cm s}^{-1}$; $v = -50.5 \pm 11.9 \text{ cm s}^{-1}$; $(v^2 + w^2)^{1/2} = 74.0 \pm 17.4 \text{ cm s}^{-1}$). The AoA during the power stroke changed from 0 to 90 degrees. Using the kinematics data and the average lift coefficient corresponding to the AoA range, we calculated the average lift-based thrust to be $4.5 \pm 1.9 \text{ mN}$ (see Supplemental information). The average ratio between lift-based thrust and required thrust was 1.2 ± 0.2 . The resulting lift-based thrust is an order of magnitude larger than the drag-based counterpart and a similar order of magnitude to the thrust required. Moreover, the temporal variation of the lift-based thrust closely follows the thrust required

independently calculated from the body kinematics (Figure 1F).

These results show that the previously overlooked lift-based thrust is the major source of the propulsive force necessary for accelerating the body and overcoming hydrodynamic drag associated with the fast aquatic locomotion of the whirligig beetles. The absence of significant backward leg movement relative to the water is likely due to the high initial swimming velocity (Figure 1G), which negates the backward leg motion. The drag-based thrust may still play a role, especially when the beetle accelerates from rest or in slow swimming. This is the case for another one-centimeter surface swimming insect, *Corixidae*, which has effective drag-based propulsion wherein $\sim 15 \text{ cm s}^{-1}$ swimming speed is achieved with $\sim 40 \text{ cm s}^{-1}$ power stroke speed (relative to body)⁶. Furthermore, while the lift-based thrust dominates the power stroke phase, the remaining 28% of the total impulse arises during the extension phase, wherein the propulsion might consist of the drag-based and other forms of hydrodynamic thrust associated with the rotation of the hind leg about the leg axis coupled with surface tension effects⁷.

The lift-based propulsion displayed by the whirligigs aligns with the broader evolutionary trend observed in larger animals. Faster-swimming marine mammals and waterfowls tend to forego drag-based thrust in favor of lift-based thrust^{8,9}. Remarkably, our results show that aquatic locomotion of one-centimeter scale whirligig beetles extends this trend down to a length scale two orders of magnitude smaller. Thus, a comparative study of whirligig beetle's hind-leg morphology and kinematics with that of other closely related aquatic beetles (e.g. *Dytiscidae*) from the perspective of drag-to-lift transition could provide valuable insights into the evolution of aquatic locomotion in beetles^{3,10}.

Whirligig beetles' efficient and explosive near surface locomotion has been inspirational for design of near surface robots and uncrewed surface vehicles⁴. The new mechanistic understanding of thrust generation could continue to inspire future designs of lift-generating surfaces, such as hydrofoils and propeller blades.

SUPPLEMENTAL INFORMATION

Supplemental information includes two figures, experimental procedures, author contributions and one video, and can be found with this article online at <https://doi.org/10.1016/j.cub.2023.11.008>.

ACKNOWLEDGEMENTS

We thank Yufan Qin, Dr. Christopher Dougherty, Dr. Sunghwan Jung, Dr. Daisuke Takagi, Dr. Sungyon Lee, Dr. Ron Hoy, Yicong Fu, Aspen Shih, and four anonymous reviewers for their valuable discussion, assistance on the experiments and comments on the manuscript. Y.S. and C.R. gratefully acknowledge the support by NSF CMMI-2042740. J.S. gratefully acknowledges the support by NSF DGE-1922551 and NSF DGE-2139899.

DECLARATION OF INTERESTS

The authors declare no competing interests.

REFERENCES

- Nachtigall, W. (1961). Funktionelle Morphologie, Kinematik und Hydromechanik des Ruderapparates von Gyrinus. Z. Vergl. Physiol. 45, 193–226.
- Voise, J., and Casas, J. (2010). The management of fluid and wave resistances by whirligig beetles. J. R. Soc. Interface 7, 343–352.
- Jami, L., Gustafson, G.T., Steinmann, T., Piñeirua, M., and Casas, J. (2021). Overcoming drag at the water-air interface constrains body size in whirligig beetles. Fluids 6, 249.
- Xu, Z., Lenaghan, S.C., Reese, B.E., Jia, X., and Zhang, M. (2012). Experimental studies and dynamics modeling analysis of the swimming and diving of whirligig beetles (Coleoptera: Gyrinidae). PLoS Comput. Biol. 8, e1002792.
- Vogel, S. (1994). Life in Moving Fluids: The Physical Biology of Flow (Princeton, NJ: Princeton University Press).
- Ngo, V., and McHenry, M.J. (2014). The hydrodynamics of swimming at intermediate Reynolds numbers in the water boatman (Corixidae). J. Exp. Biol. 217, 2740–2751.
- Hu, D., and Bush, J. (2010). The hydrodynamics of water-walking arthropods. J. Fluid Mech. 644, 5–33.
- Fish, F.E. (1996). Transitions from drag-based to lift-based propulsion in mammalian swimming. Am. Zool. 36, 628–641.
- Johansson, L.C., and Norberg, R.Å. (2003). Delta-wing function of webbed feet gives hydrodynamic lift for swimming propulsion in birds. Nature 424, 65–68.
- Liu, S.-P., Wipfler, B., and Beutel, R.G. (2018). The unique locomotor apparatus of whirligig beetles of the tribe Orectochilini (Gyrinidae, Coleoptera). J. Zool. Syst. Evol. Res. 56, 196–208.

¹Biological and Environmental Engineering, Cornell University, Ithaca, NY 14853, USA.

²Applied and Engineering Physics, Cornell University, Ithaca, NY 14853, USA.

E-mail: ys655@cornell.edu (Y.S.); jls627@cornell.edu (J.S.); cr296@cornell.edu (C.R.)